Cerebral Cortex, 2017; 1–14

doi: 10.1093/cercor/bhx253
Original Article

ORIGINAL ARTICLE

Latent-Profile Analysis Reveals Behavioral and Brain Correlates of Dopamine-Cognition Associations

Martin Lövdén[1], Nina Karalija[2,3], Micael Andersson[3,4], Anders Wåhlin[2], Jan Axelsson[2,3], Ylva Köhncke[1], Lars S. Jonasson[2,3,5], Anna Rieckman[2,3], Goran Papenberg[1], Douglas D. Garrett[6,7], Marc Guitart-Masip[1], Alireza Salami[1], Katrine Riklund[2,3], Lars Bäckman[1], Lars Nyberg[2,3,4] and Ulman Lindenberger[6,7,8]

[1]Aging Research Center, Karolinska Institutet and Stockholm University, Stockholm, Sweden, [2]Department of Radiation Sciences, Umeå University, Umeå, Sweden, [3]Umeå Center for Functional Brain Imaging (UFBI), Umeå University, Umeå, Sweden, [4]Department of Integrative Medical Biology, Umeå University, Umeå, Sweden, [5]Center for Aging and Demographic Research, CEDAR, Umeå University, Umeå, Sweden, [6]Max Planck UCL Centre for Computational Psychiatry and Ageing Research, Berlin, Germany, [7]Center for Lifespan Psychology, Max Planck Institute for Human Development, Berlin, Germany and [8]European University Institute, San Domenico di Fiesole (FI), Italy

Address correspondence to Martin Lövdén Aging Research Center, Karolinska Institutet, Gävlegatan 16, 113 30 Stockholm, Sweden. Email: Martin.Lovden@ki.se

Abstract

Evidence suggests that associations between the neurotransmitter dopamine and cognition are nonmonotonic and open to modulation by various other factors. The functional implications of a given level of dopamine may therefore differ from person to person. By applying latent-profile analysis to a large (n = 181) sample of adults aged 64–68 years, we probabilistically identified 3 subgroups that explain the multivariate associations between dopamine $D_{2/3}$R availability (probed with ^{11}C-raclopride-PET, in cortical, striatal, and hippocampal regions) and cognitive performance (episodic memory, working memory, and perceptual speed). Generally, greater receptor availability was associated with better cognitive performance. However, we discovered a subgroup of individuals for which high availability, particularly in striatum, was associated with poor performance, especially for working memory. Relative to the rest of the sample, this subgroup also had lower education, higher body-mass index, and lower resting-state connectivity between caudate nucleus and dorsolateral prefrontal cortex. We conclude that a smaller subset of individuals induces a multivariate non-linear association between dopamine $D_{2/3}$R availability and cognitive performance in this group of older adults, and discuss potential reasons for these differences that await further empirical scrutiny.

Key words: Cognitive Performance, dopamine $D_{2/3}$ Receptor Availability, Heterogeneity, Latent Profile Analysis, Older Adults, Working Memory

Introduction

The neurotransmitter dopamine plays an important but complex role in several cognitive processes (Liggins 2009; Shohamy and Adcock 2010; Cools and D'Esposito 2011; Lisman et al. 2011, for reviews). In line with this evidence, we recently reported that between-person differences in striatal and hippocampal dopamine D_2 and D_3 receptor ($D_{2/3}R$) availability were linearly and positively associated with episodic memory performance in a large cohort of older adults (Nyberg et al. 2016). However, we observed no such association with working memory performance. Though D_1 receptors have been more directly implicated in working memory processes (Arnsten et al. 1994; Liggins 2009; Rieckmann et al. 2011; Roffman et al. 2016), there are reasons for also expecting a role of D_2 receptors. For example, D_2 receptor agonists and antagonists affect aspects of human working memory performance (e.g., Luciana et al. 1992; Mehta et al. 2004; van Holstein et al. 2011), perhaps partly through the involvement of the hippocampus (Takahashi et al. 2008; Liggins 2009; Takahashi 2013). Animal work implicates frontal D_2 receptors in attentional and flexibility-based aspects of working memory (Floresco et al. 2006; Puig and Miller 2015; Ott and Nieder 2017). In addition, biophysically grounded computational models suggest a role of cortical D_2 receptors in the flexible switching between representational states in working memory (Durstewitz and Seamans 2008; Rolls et al. 2008). D_2 receptors may also be involved in striatal-based selective updating of working memory (Frank et al. 2001; Mehta et al. 2004; Bäckman et al. 2011). Thus, it remains plausible that between-person differences in dopamine $D_{2/3}R$ availability relate to working memory performance under specific constraints that may not have been captured in our previous work (Nyberg et al. 2016).

One possibility is that associations between inter-individual differences in dopamine $D_{2/3}R$ availability and working memory emerge in both non-linear and multivariate ways, such that certain levels of regional dopamine $D_{2/3}R$ availability result in different behavioral outcomes for different individuals depending on the state of the rest of their neural system. Similar to dopamine D_1 receptor activation (Arnsten 1997; Zahrt et al. 1997; Cools and D'Esposito 2011), D_2 receptor activation may nonmonotonically relate to working-memory processes (Floresco 2013). In addition, examples such as the upregulation of prefrontal dopamine in early Parkinson's disease (Rakshi et al. 1999) point to the importance of multivariate individual patterns. For example, in the presence of low striatal dopamine availability, high cortical availability may have different functional consequences than it has in the presence of high striatal availability. In line with this view, some trains of thought suggest that low striatal dopamine levels may result in lower probability of gating information into working memory, and that having a robust signal in prefrontal cortex in this situation may cause difficulties in updating working memory representations (Frank et al. 2001; Cools and D'Esposito 2011; D'Ardenne et al. 2012).

Adding to this complexity, expectations based on experimental and theoretical work on within-person differences may, due to sample heterogeneity, not play out in between-person differences (Kievit et al. 2013; Schmiedek et al. 2016). Sample heterogeneity may result in associations among variables in the overall sample that may differ markedly from the associations observed within some or all of the subgroups. The literature suggests a presence of such heterogeneity that may distort bivariate dopamine-cognition associations. Whereas striatal dopamine $D_{2/3}R$ availability is substantially decreased in older adults (Bäckman et al. 2010), other groups of individuals that also on average show reduced cognitive performance, in particular reduced working memory and executive control, may display high striatal dopamine $D_{2/3}R$ availability (e.g., schizophrenia: Rolls et al. 2008; Howes and Kapur 2009; ADHD: Badgaiyan et al. 2015; overweight: Cosgrove et al. 2015; Horstmann et al. 2015; Dang et al. 2016). High striatal $D_{2/3}R$ availability may thus signal low or high functioning in different subgroups of individuals—a pattern of heterogeneity that is difficult to detect with either normal linear or classic nonlinear bivariate statistics across the entire group.

Here, we apply latent-profile analysis to represent the presence of subgroups that may account for the multivariate associations between dopamine $D_{2/3}R$ availability (assayed with ^{11}C-raclopride-PET at rest) and cognitive performance in a large (n = 181) sample of older adults (age = 64–68 years). Grounded in the multivariate perspective, we included cortical, striatal, and hippocampal dopamine $D_{2/3}R$ availability and several key aspects of cognitive performance (episodic memory, working memory, and psychomotor speed) that have been linked to dopamine (e.g., Backman et al. 2006; Cools and D'Esposito 2011; Lisman et al. 2011).

Latent-profile analysis is a type of Gaussian mixture modeling that probabilistically represents the presence of subgroups (i.e., multiple multivariate Gaussians) in multivariate data with a latent (i.e., unobserved) variable. Similar to other unsupervised statistical-learning techniques such as cluster analysis, it is typically set up so that multivariate associations in the data are accounted for by forming subgroups of subjects that are described by their mean profiles in the variables analyzed. That is, the typical model assumes that the existence of the classes is the reason why the variables are correlated. With the appropriate number of classes, correlations among variables within classes are thus not present. Thus, latent-profile analysis is well suited for describing, in a data-driven manner, non-linear multivariate patterns of individual differences in cognitive performance and dopamine $D_{2/3}R$ availability. Its probabilistic feature, with each individual having a probability of belonging to each of the classes, allows for characterizing the discovered groups on other variables without assuming absolute group membership (and thus high classification accuracy) for the individuals. This aspect is important, because differences among classes may critically inform interpretation. Based on the results of the latent-profile analysis, we probed differences among the classes on select aspects of the rich set of demographic, health, genetic, and structural and functional magnetic resonance imaging (MRI) measures that are available for this sample. Although advantageous in many ways, this statistical approach, including both the profile analysis and the investigation of differences between classes, is exploratory in nature. The need for future confirmatory studies should therefore be kept in mind when interpreting results.

Materials and Methods

This study uses data from the Cognition, Brain, and Aging (COBRA) project. A detailed description of the recruitment procedure, imaging protocols, and cognitive and life-style assessments in the COBRA study has been previously published (Nevalainen et al. 2015). Here, we describe the methods directly relevant to the present results.

Participants

The sample consisted of 181 older individuals (64–68 years; mean = 66.2, SD = 1.2; 81 women) randomly selected from the

population register of Umeå, in northern Sweden. Exclusion criteria included suspected brain pathology, impaired cognitive functioning (Mini Mental State Examination <27), and conditions that could bias the measurements of cognitive performance (e.g., severely reduced vision) or hinder imaging (e.g., metal implants). About 22% of the sample was working, 18% used nicotine, and 33% took blood pressure medications. Mean education was 13.3 years (SD = 3.5), Body-Mass Index (BMI) was 26.1 (SD = 3.5), systolic blood pressure was 142 (SD = 17), and diastolic blood pressure was 85 (SD = 10). The sample is fairly representative of the healthy target population in Umeå (Nevalainen et al. 2015).

Image Acquisition

MR imaging was performed with a 3 tesla Discovery MR 750 scanner (General Electric), equipped with a 32-channel phased-array head coil. Positron Emission Tomography (PET) was done with a Discovery PET/CT 690 scanner (General Electric).

PET Image Acquisition

PET was performed during resting-state conditions following an intravenous bolus injection of 250 MBq ^{11}C-raclopride. Preceding the injection, a low-dose helical CT scan (20 mA, 120 kV, 0.8 s/revolution) was obtained to be used for attenuation correction. Starting at tracer injection, a 55-min 18-frame dynamic scan was acquired (9 × 120 s + 3 × 180 s + 3 × 260 s + 3 × 300 s). Attenuation, scatter and decay- corrected images (47 slices, axial field of view = 25 cm, 256 × 256-pixel transaxial images, voxel size = 0.977 × 0.977 × 3.27 mm) were reconstructed with the resolution-recover Ordered Subset Expectation Maximum (OSEM) iterative algorithm VUE Point HD-SharpIR (Bettinardi et al. 2011). The reconstruction was performed using 6 iterations, 24 subsets, and 3.0 mm post filter, yielding a full width at half maximum (FWHM) resolution of approximately 3.2 mm (Wallsten et al. 2013). A second image set was reconstructed using Filtered Back Projection (FBP) with a 6.4 mm post-filter, to the same matrix size. Head movements during the imaging session were minimized with an individually fitted thermoplastic mask that was attached to the bed surface.

Structural MRI

A 3D fast spoiled-echo sequence was used for acquiring anatomical T1-weighted images, collected as 176 slices with a thickness of 1 mm., TR = 8.2 ms., TE = 3.2 ms., flip angle = 12 degrees, and field of view = 25 × 25 cm. White-matter microstructure was examined using diffusion tensor imaging (DTI). These images were acquired by a spin-echo-planar T2-weighted sequence, using 3 repetitions and 32 independent directions. The total slice number was 64, with a TR of 8000 ms, a TE of 84.4 ms, a flip angle of 90 degrees, a field of view of 25 × 25 cm, and with b = 1000 s/mm^2. Perfusion measurements were made with a whole-brain 3D pseudo-continuous arterial-spin labeling (ASL), with background suppression and a spiral acquisition scheme. Additional parameters were: Labeling time = 1.5 s, post labeling delay = 1.5 s, field of view = 24 cm, slice thickness = 4 mm, and resolution = 8 arms by 512 data points, 30 control/label pairs, 3 signal averages, TR = 4674 ms, TE = 10 ms, field of view = 240 × 240 mm A FLAIR sequence was acquired to assess white-matter hyperintensities. The total number of slices were 48, with a slice thickness of 3 mm. TE was 120 ms, TR was 8000 ms, and field of view was 24 × 24 cm.

Functional MRI

BOLD-contrast sensitive scans where acquired using a T2*-weighted single-shot gradient echoplanar imaging sequence. Parameters were 37 transaxial slices, 3.4 mm thickness, 0.5 mm spacing, TE/TR = 30/2000 ms, 80 degrees flip angle, 25 × 25 cm field of view, and a 96 × 96 acquisition matrix. At the start of the scan, 10 dummy scans were collected. The functional data were acquired during resting-state conditions (6 min) and during a working memory task (numerical n-back). In this task, a sequence of single numbers appeared on the screen. Each number was shown for 1.5 s, with an ISI of 0.5 s. During each item presentation, participants reported if the number currently seen on the screen was the same as 1, 2, or 3 digits back. A heading that preceded each subtest indicated the actual condition. Participants responded by pressing 1 of 2 adjacent buttons with the index or middle finger to reply "yes, it is the same number" or "no, it is not the same number", respectively. A total of 9 blocks for each condition (1-, 2-, and 3-back) was performed in random order, each block consisting of 10 trials. The trial sequence was the same for all participants.

Image Processing

PET Images

To generate regions of interests (ROIs) for the PET images, we parcellated cortical and subcortical brain regions on the T1-weighted images, using FreeSurfer 5.3 (http://surfer.nmr.mgh.harvard.edu/). This process relies on atlas-based probabilistic models of characteristic magnetic-resonance appearances and spatial relationships (Fischl et al. 2002; Desikan et al. 2006). A supercomputer cluster, Abisko, located at Umeå University, was used for data processing. The following command line statement was used "recon-all -s $AnatomicalFile -sd $SubjectDirectory -all -qcache -hippo-subfields -nuintensitycor-3 t -schwartzya3t-atlas".

The PET emission scan format was converted from DICOM to NIfTI, corrected for head movements, and then co-registered to the corresponding T1-weighted images using Statistical Parametric Mapping software (SPM8). Binding potential, defined as the ratio of specifically bound radioligand to non-displacable radioligand in tissue (BP_{ND}; (Innis et al. 2007), was calculated from the time-activity curves for each ROI emanating from the cortical and subcortical parcellation described above using Reference Logan analysis (Logan et al. 1996). The regression for determining the slope from the Logan analysis started from 18 minutes post injection, after which the Logan plot followed a straight line. Cerebellum was used as reference region, because of its negligible $D_{2/3}$R expression (Farde et al. 1986; Levey et al. 1993).

BP_{ND} was calculated using the above-mentioned procedure on both Sharp-IR and FBP-reconstructed images. Sharp-IR reconstruction has ~3 mm FWHM resolution, and is therefore superior when examining small or narrow features, but is known to exhibit bias for low-intensity regions (Walker et al. 2011; Jian et al. 2015). Therefore, FBP reconstruction was used to independently quantify BP_{ND}-values in extrastriatal regions where $D_{2/3}$R availability is low. The BP_{ND} values did however correlate to a high degree for the two reconstruction methods for all ROIs included in the analyses of this paper (r-values: mean = 0.90, median = 0.91, min. = 0.70, max. = 0.97; $P < 0.001$ for all), and we chose therefore to perform all analyses on Sharp-IR reconstructed data.

Although it is uncommon to measure extrastriatal dopamine $D_{2/3}$R availability with ^{11}C-raclopride-PET, recent evidence indicates good reliability of such measures (Alakurtti et al. 2015). In line with this evidence, analyses of the present data showed

that median BP_{ND} was significantly higher in all ROIs than in the cerebellar reference region, with the left frontal pole showing the smallest difference from the cerebellar reference area (mean $BP_{ND} = 0.1$; $t = 15$, $p < .001$). Moreover, confirmatory factor modeling on the present dataset has shown strong positive links between BP_{ND} in the ROIs across the hemispheres and among different brain regions that tap known anatomical dopamine subsystems, and less strong associations between regions of different subsystems (Papenberg et al. 2017), supporting a division into cortical, striatal, and limbic factors for the purpose of the current study. Thus, we deem the extrastriatal estimates as reliable and reflective of target binding.

Dopamine $D_{2/3}R$ BP_{ND} was missing for 4 participants due to imperfect segmentation of MR images or PET/MR co-registration. Three statistical outliers in striatal $D_{2/3}R$ BP_{ND} (outlier labeling rule with 2.2 interquartile ranges; Hoaglin and Iglewicz 1987) were deleted. Five statistical outliers were detected in the cortical BP_{ND} data and these scores were deleted. BP_{ND} were then averaged across left and right striatum and left and right hippocampus. These variables were then standardized (mean = 0; SD = 1) to form the measures of striatal and hippocampal dopamine $D_{2/3}R$ availability. Cortical dopamine $D_{2/3}R$ availability was represented in analyses with the standardized first principal component from a factor analysis of BP_{ND} in all cortical ROIs. This first principal component accounted for 40.5% of the variance in cortical availability.

Volumetric MRI Processing

To quantify gray-matter volumes, T1-weighted images were first segmented into gray matter, white matter, and cerebrospinal fluid using the unified segmentation approach (Ashburner and Friston 2005) in SPM12b (Statistical Parametric Mapping, Wellcome Trust Centre for Neuroimaging, http://www.fil.ion.ucl.ac.uk/spm/) implemented in Matlab 10 (The Mathworks, Inc). Moreover, the "light clean up" option was used to remove odd voxels from the segments. The gray-matter images were further analyzed using DARTEL (Ashburner 2007) in SPM12b (Diffeomorphic Anatomical Registration Through Exponentiated Lie Algebra). The gray-matter segments were imported into DARTEL space, and a final customized template was created as well as subject-specific flow fields containing the individual spatial-normalization parameters (diffeomorphic nonlinear image registration). Gray-matter segments were further warped into standard MNI space, by incorporating an affine transformation mapped from the DARTEL template to MNI space. In addition, the normalized gray-matter volumes were modulated by scaling them with Jacobian determinants from the registration step to preserve local-tissue volumes. Volumes were smoothed with a FWHM Gaussian kernel of 8 mm in the 3 directions. Here, we focused on the measure of total gray-matter volume, corrected for intracranial volume (gray matter + white matter + cerebrospinal volume; ICV) using the analysis of covariance approach: adjusted volume = raw volume - b(ICV – mean ICV), where b is the slope of regression of volume on ICV (Raz et al. 2005). To complement this measure, we also extracted mean-modulated striatum volumes from each individual's smoothed images based on the masks of the striatum (caudate and putamen) from the WFU Pickatlas. These measures were also corrected for ICV and averaged across hemispheres to form one measure of striatal volume.

Perfusion Analyses

Quantitative perfusion maps (in ml/100 g/min) were calculated using a post-processing tool installed on the scanner by the manufacturer. The perfusion maps where normalized to MNI space using the DARTEL-derived transformation fields and affine registration. Gray matter perfusion was calculated by averaging perfusion over voxels with a gray-matter probability higher than 25% in the group template.

Diffusion-Weighted Image Processing

Diffusion-weighted data analysis was performed using the University of Oxford's Center for Functional Magnetic Resonance Imaging of the Brain (FMRIB) Software Library (FSL) package (http://www.fmrib.ox.ac.uk/fsl) and Tract-Based Spatial Statistics (TBSS) as part of the FMRIB software package. The full details of DTI data analyses (using identical imaging parameters, but in a different sample) are given elsewhere (Salami et al. 2012). In short, the 3 subject-specific diffusion acquisitions were concatenated in time followed by eddy-current correction to adjust for head motion and eddy-current distortions. Accordingly, the *b*-matrix was reoriented based on the transformation matrix (Leemans and Jones 2009). Next, the first volume within the averaged volume that did not have a gradient applied (i.e., the first $b = 0$) was used to generate a binary brain mask with the Brain Extraction Tool (Smith 2002). Finally, DTIfit was used to fit a diffusion tensor to each voxel included in the brain mask/space. As such, voxel-wise maps of fractional anisotropy (FA) were generated. Using the TBSS processing stream, all subject-specific FA maps were nonlinearly normalized to standard space (FMRIB58_FA) and then fed into a skeletonize program to make a skeleton of common white-matter tracts across all subjects. Mean diffusivity (MD) images were processed based on the results of the processing of the FA images, yielding individual MD skeletons. Averaged FA and MD along the spatial course of the entire skeleton and of seven major WM tracts (genu, body, splenium, fornix, superior longitudinal fasciculus, superior fronto-occipital fasciculus, and cingulum) were computed with reference to JHU ICBM-DTI-81 white matter labels (Wakana et al. 2004).

Segmentation of White-Matter Hyperintensities

Lesions were segmented by the lesion growth algorithm (Schmidt et al. 2012) as implemented in the LST toolbox version 2.0.14 (www.statisticalmodelling.de/lst.html) for SPM12. The algorithm first segmented the T1 images into the 3 main tissue classes (cerebrospinal fluid, gray matter, and white matter). Following, this information was combined with the coregistered FLAIR intensities to calculate lesion belief maps. By thresholding these maps with a pre-chosen initial threshold ($\kappa = 0.3$, defined by visual inspection), an initial binary lesion map was obtained. This initial map was then grown along neighboring voxels that appeared hyperintense in the FLAIR image, resulting in a lesion probability map. Finally, the lesion probability map was thresholded (threshold: 50%) to obtain the binary map of lesions. From these, the total volume (cm^3) of white-matter lesions per individual were attained.

Functional MRI Analyses

SPM8 (Wellcome Department of Cognitive Neurology, London, UK) was used for preprocessing and data analysis of the fMRI task and resting state data. Preprocessing of the task fMRI data included slice-timing correction, unwarping and realignment of the time-series to the first image of each volume, and normalization to a sample-specific template (using DARTEL), followed by affine alignment to MNI standard space. Data were resampled to 2-mm isotropic voxels and spatially smoothed using an 6-mm FWHM Gaussian kernel. First-order task

analyses included the experimental conditions (1-back, 2-back, 3-back) as regressors of interest in a general linear model, convolved with a hemodynamic response function. The six realignment parameters were included as covariates of no interest to account for residual movement artifacts.

In order to obtain measures of fronto-parietal upregulation of brain activity across load in the 1-back to the 2-back and 3-back working memory tasks, fMRI contrast estimates (betas) were extracted from the relevant contrast images (1-back <2-back, 1-back <3-back), averaged across 9 regions of the core frontoparietal WM network (Fig. 3; anterior cingulate, bilateral anterior prefrontal cortex, bilateral dorsolateral prefrontal cortex (DLPFC), bilateral anterior insula, and bilateral anterior inferior parietal cortex). Because fMRI estimates were extracted both from task and resting state, ROIs were selected a priori as 5 mm spheres around the fronto-parietal control network seeds as described by Vincent et al. (2008).

Preprocessing of the resting state data was carried out using the Data Processing Assistant for Resting-State fMRI (Chao-Gan and Yu-Feng 2010). Data were corrected for acquisition time differences between slices within each volume and then motion corrected. A within-subject rigid registration was carried out to align functional and structural T1-weighted images. Next, the effect of physiological noise was removed by regressing out Friston's 24 parameters from a motion model (Yan et al. 2013), as well as nuisance variables, such as global signal, white matter, and cerebrospinal fluid signal, along with both linear and quadratic trends. In addition, nuisance-corrected data were bandpass filtered (passband 0.01–0.1 HZ). Finally, using DARTEL, the noise-corrected realigned fMRI images were nonlinearly normalized to the sample-specific group template, affine aligned into stereotactic MNI space, and smoothed using a 6.0-mm FWHM Gaussian filter.

Previous findings have demonstrated functional relationships between dorsal caudate and several parts of the fronto-parietal circuitry (Postuma and Dagher 2006; Di Martino et al. 2008). To obtain a finer parcellation of the caudate, Martino et al. distinguished ventral caudate (VC) from dorsal caudate (DC) based on the Z coordinate following Postuma and Dagher (2006). We followed closely the approach taken by Martino et al. and placed seeds in each hemisphere (DC: ±13 15 9). Then, a 4 mm diameter sphere centered on the aforementioned coordinates was generated and the mean time series was computed by averaging across voxels for each seed. For both hemispheres, multiple regression analyses were carried out for each subject including the time series of a seed, yielding subject-specific functional connectivity maps of each seed. Functional connectivity maps for each subject were taken into a second-level multiple-regression analysis to delineate regions that are functionally connected to each seed at the group level. Local maxima with $P < 0.05$ (FWE-corrected), with an extent threshold of 10 continuous voxels ($k > 10$) were considered to be statistically significant. Then, we overlapped the seed regions from Vincent et al. (2008) with the functional connectivity map of the left and right DCs and computed the average correlation between left and right DC and each fronto-parietal seed.

Cognitive Measures

Episodic memory, working memory, and psychomotor speed were assessed with 3 tasks each (1 verbal, 1 numerical, and 1 figural task per ability). Episodic memory was measured with word recall, number-word recall, and object-position recall. Working memory was assessed with letter updating, columnized numerical 3-back, and spatial updating. Speed was tested with letter comparison, number comparison, and figure comparison (see Nevalainen et al. 2015, for details). Task scores were computed by summing performance across blocks or trials of each task. Confirmatory factor modeling has shown that these task scores can be used to form a model of working memory, episodic memory, and psychomotor speed that fits the data well (Nevalainen et al. 2015). We therefore standardized and averaged the 3 task-scores of each ability to create 1 unit-weighted measure for each of the 3 cognitive abilities. In case of missing data (<1.2% for all variables, with technical errors or misunderstandings of the task accounting for almost all of these missing data points), an average of the available observed scores for a cognitive ability was imputed into these ability measures, so that these variables do not have missing values. This approach corresponds to a regression imputation assuming equal loadings of the tasks on the latent ability they are assumed to measure. Standardized (z-scores; mean = 0; SD = 1) versions of these unit-weighted averages were used in the analyses.

Health Variables

Objective health measures included BMI and blood pressure measurements. Subjective reports of medication use formed the basis for dichotomous variables representing use of medication for indications of hyperlipidemia, atherosclerosis, cardiovascular disease, hypertension, and depression/anxiety. A dichotomous measure of high blood pressure was formed by a combination of either the blood pressure measurements (systolic > 140; diastolic > 90) or self-reported use of blood pressure medication.

Leisure Activities and Personality

Self-reported leisure activities were assessed using a questionnaire that included 43 activities, 18 intellectual, 15 physical, and 10 social. Participants were asked to indicate for how many hours (1, 2, 3, etc., 15+h) they engage in each of the activities during a typical summer week. A sum score (hours/week) was computed across all intellectual, physical, and social activities, respectively. Outliers (>3.29 SD) were excluded variable-wise ($n = 2$ from intellectual activities, $n = 1$ from physical activities, $n = 2$ from social activities). In addition to frequency of each activity, the questionnaire asked for intensity ratings for each of the intellectual and physical activities. For each intellectual activity, participants were asked to rate how mentally demanding it would normally be to perform the activity (on a scale from 1 = "not at all" to 5 = "extremely"). For each physical activity, they were asked how physically demanding the activity would be (1–5). A mean across intensity ratings was computed for intellectual and physical activities, respectively. A rating was included in the mean score only if the rater had also reported at least 1 hour/week of engagement in a given activity.

Genetics

Blood samples were analyzed for presence of single-nucleotide polymorphisms (SNPs) in genes for the D2 receptor (C957T; rs6277), Catechol-O-Methyltransferase (COMT; rs4680), dopamine- and cAMP-regulated neuronal phosphoprotein (DARPP-32, PPP1R1B; rs879606), and the vesicular monoamine transporter 2 (VMAT2, SLC18A2; rs363387). These SNPs were chosen as they likely entail differences in dopamine transmission, via proteins that regulate striatal and frontal dopamine levels, dopamine

signaling, and vesicular dopamine storage (Lachman et al. 1996; Hirvonen et al. 2004; Schwab et al. 2005; Kunii et al. 2014). They have furthermore been associated with behavioral differences, including working memory performance (Meyer-Lindenberg et al. 2007; Diaz-Asper et al. 2008; Lindenberger et al. 2008; Colzato et al. 2016).

Based on previous literature, allelic variants were categorized as markers of a beneficial (C-allele of C957T, A-allele carriers of COMT, G homozygotes for DARPP-32, and G-allele carriers of VMAT2) or less beneficial (T homozygotes of C957T, G homozygotes of COMT, A-allele carriers of DARPP-32, and T homozygotes of VMAT2) dopamine signaling profile, and scored 1 or 0 accordingly. Thus, the summarized gene score ranged between 0 and 4. Furthermore, Apolipoprotein E gene polymorphisms (ApoE, rs7412, and rs429358) were also analyzed, and the distribution of carriers versus non-carriers of the ε4 allele was compared between classes. This is motivated by the ApoE ε4 allele being a strong predictor of cognitive decline in aging (Christensen et al. 2008; Schiepers et al. 2012).

Upon analysis, deoxyribonucleic acid (DNA) was extracted from the buffy-coat fraction of blood samples using the Kleargene™ XL nucleic acid extraction kits and genotyping of SNPs was carried out with KASP™ genotyping assays (at LGC genomics). In brief, DNA template was mixed with a KASP master mix (containing KASP Taq polymerase, deoxynucleoside triphosphates, buffers, salts, 2 fluorescently-labeled (FAM and HEX) reporter cassettes), and a SNP-specific KASP Assay mix (containing 2 allele-specific forward primers and one common reverse primer). Then, polymerase chain-reaction sessions were performed, during which primers bound to their target sequences, fluorophores were incorporated into the DNA product, and the DNA product was amplified. SNP allelic variants were determined via detection of FAM or HEX fluorescence for homozygous alleles, or both for heterozygous alleles.

For each analysis, 2 forward and 1 reverse primers were constructed. The forward primers differed at one base in the 3′-end and included 5′-CA TGG TCT CCA CAG CAC TCC C/T-3′ for rs6277, 5′-GCA TGC ACA CCT TGT CCT TCA C/T-3′ for rs460, 5′-G GGA AAG GGT GGC AGG AGG T/C-3′ for rs879606, and 5′-GC CAG GCC AGT GCA CAC G/T-3′ for rs363387. Reverse primers used were 5′-TCT CRG GTT TGG CGG GGC TGT-3′ for rs6277, 5′-CAT CAC CCA GCG GAT GGT GGA T-3′ for rs460, 5′-AGG ACA TCC CAC TCC TAT GAG CAA-3′ for rs879606, and 5′-AGA TGC TCT GGA AGC TGT CTG AGA T-3′ for rs363387.

Statistical Procedures

A series of latent-profile (mixture) models from 1 to 4 classes were conducted for representing the presence of latent subgroups (multiple multivariate Gaussians) of cognitive (episodic memory, working memory, and psychomotor speed) performance and dopamine $D_{2/3}R$ availability in the striatum, hippocampus, and neocortex that account for the multivariate associations among the variables. All analyses were performed with Mplus 7.4 (Muthén and Muthén 2015). In these analyses, scattered missing values (on the measures of dopamine $D_{2/3}R$ availability) are accommodated in the Mplus estimation under the missing-at-random assumption. Classes (i.e., subgroups) were assumed to have equal variances. As is typical for these analyses, we did not allow for residual covariances between observed variables within classes (i.e., we assumed local independence), because we aimed at explaining the multivariate associations based on the formation of classes. That is, our model assumes that the presence of latent classes is the reason that the variables are correlated. With the appropriate number of classes, correlations among variables within classes are not present and all information about the associations among variables can be found by inspecting the differences among classes in their mean profile on the variables of interest.

The Bayesian Information Criterion (BIC) was used as the primary method to select the best-fitting model (i.e., the number of classes). A lower BIC indicates a model with better fit and parsimony. A bootstrapped Lo-Mendell Rubin Test (BLRT) of the difference in fit between a model with k classes and one with k-1 classes (2*ΔLL, ΔDF) was used to further inform model selection in case the BIC comparison was ambiguous. Standardized entropy (ranging from 0 to 1) was used to measure classification accuracy.

After determining the number of classes, interpretation of the results was based on profiling the means of the latent classes. Based on these results, we then examined differences among the classes on select aspects of the available demographic, lifestyle, health, genetic, and functional and structural brain variables. We selected those aspects that we considered as potentially informative correlates of the association between dopamine $D_{2/3}R$ availability and cognitive performance revealed by the latent-profile results. These differences were estimated and statistically tested with the BCH (for continuous variables) and the DCAT (for categorical variables) methods implemented in Mplus 7.4. The BCH method is a 3-step method that first builds the latent class model, then determines class membership, and then tests for equality of means across classes on distal variables not included in the first step. It assumes normality and involves performing weighted statistical tests of mean differences, with weights that are inversely related to classification error probabilities. The method has been shown to perform well (Bakk and Vermunt 2015). In the DCAT method (Lanza et al. 2013), which is suitable for categorical data, Bayes theorem is used to represent joint distribution of the latent class variable and the distal variable as regression of the latent class variable conditional on the distal variable. These methods do not affect the original latent-class solution. Both take into account the probabilistic class membership of each individual. In this way, the interpretability of these results does not depend on high classification accuracy.

We aimed for a comprehensive and global description of the classes, without making strong claims regarding the nature of the classes based on single findings of statistically significant differences, and therefore set a rather lenient threshold for statistical significance at $P < .05$. In the results, we also note which findings that survive more conservative thresholds based on correction for multiple testing.

Results

Latent-Profile Analyses

Latent-profile models specifying 1, 2, 3, or 4 classes for cognitive (episodic memory, working memory, and psychomotor speed) performance and BP_{ND} in striatum, hippocampus, and cortex were estimated. The model fit indices are reported in Table 1. Our primary measure for selecting the number of classes (the BIC) had a clear minimum at 3 classes and we therefore considered this solution as the best fit to the data. Figure 1 depicts the profiles of mean cognitive performance and BP_{ND} for the 3 subgroups that this model represents. Profiles for the 2 and 4 class solutions are reported in Supplementary Materials 1.

Class 1 ($n = 99$; 55% of the sample) is a large group of individuals that generally performs above the mean of the sample

and has slightly above-average dopamine $D_{2/3}R$ availability. Class 2 (n = 42; 23%) is a group that clearly performs lower than the class 1 and has low BP_{ND} in all regions. In contrast to this class of individuals with low dopamine $D_{2/3}R$ availability and performance, class 3 (n = 40; 22%) displays high dopamine $D_{2/3}R$ availability (especially in striatum, where it is even higher than for class 1) despite low cognitive performance, especially for working memory where they perform lower than class 2. In other words, the multivariate associations in the data are accounted for by forming classes of subjects indicating that relatively high $D_{2/3}R$ availability is associated with high cognitive performance for most individuals, but that there is a smaller group of individuals where high availability, particularly in striatum, instead is associated with poor performance, especially for working memory.

Table 1 Model fit indices

	One Class	Two Classes	Three Classes	Four Classes
Log-Likelihood	−1518	−1484	−1460	−1448
BIC	3099	3066	3055	3068
Entropy		0.64	0.70	0.73
2*ΔLL (ΔDF)		69(7)	47(7)	24(7)
BLRT approx. p-value		<0.0001	<0.0001	0.0400

Note. BIC, Bayesian Information Criterion; ΔLL = Difference in log-likelihood between a model with k classes and one with k-1 classes; BLRT = Bootstrapped Lo-Mendell Rubin Test.

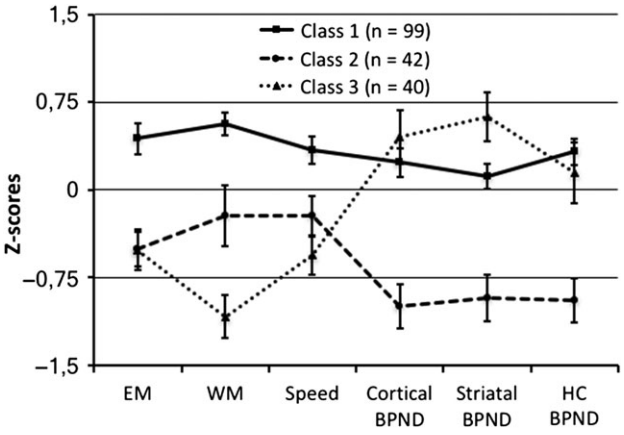

Figure 1. Mean (SE) profiles of cognitive performance and ^{11}C-raclopride BP_{ND} for the 3-class solution. EM, episodic memory; WM, working memory; HC, hippocampus.

Demographic and Health Differences Across Classes

To aid interpretation of the multivariate associations between dopamine $D_{2/3}R$ availability and cognitive performance that the observed classes represent, it is reasonable to first examine whether they relate to differences in more general demographic and health variables. Of the examined variables (see Table 2), 2 tended to distinguish class 3 from the other 2 classes: Individuals in class 3 had on average fewer years of education (class 3 vs. 1: $\chi^2(1) = 18.7$, $P < .001$. Class 3 vs. 2: $\chi^2(1) = 4.0$, $P = .045$) and higher BMI (class 3 vs. 1: $\chi^2(1) = 4.3$, $P = .038$. Class 3 vs. 2: $\chi^2(1) = 6.1$, $P = .013$). Individuals in class 3 in addition tended to report performing physical activities with lower intensity (class 3 vs. 1: $\chi^2(1) = 7.5$, $P = .006$; Class 3 vs. 2: $\chi^2(1) = 2.4$, $P = .119$) than the other classes. There were no statistically significant differences in sex distribution, but class 1 was younger than class 2, although this difference was very small (6 months). There were no statistically significant differences in other physical health measures, including blood pressure, medication use (including depression and anxiety medication, which was low), and nicotine consumption. In summary, class 3, with low cognitive performance despite high dopamine $D_{2/3}R$ availability, differentiates itself from the other classes mainly by consisting of individuals with higher BMI and lower education. Note however that with strict Bonferroni correction for multiple testing (0.05/57 test ≈ 0.001) only the difference

Table 2 Differences among classes on demographic, health, lifestyle, genetic, and personality variables

	Class 1	Class 2	Class 3	*P*-value for equivalence of means		
				1 vs. 2	1 vs. 3	2 vs. 3
Age (years)	66.0	66.5	66.3	0.046*	0.230	0.534
Women	46%	32%	58%	0.258	0.491	0.180
Education (years)	14.3	13.0	11.2	0.114	<0.001*	0.045*
Working	28%	12%	20%	0.087	0.519	0.616
Body-Mass Index	25.8	25.3	27.7	0.464	0.038*	0.013*
Nicotine use	15%	32%	9%	0.096	0.614	0.107
Systolic blood pressure	141	141	144	0.984	0.469	0.545
Diastolic blood pressure	86	83	85	0.305	0.753	0.509
Blood pressure med.	32%	37%	32%	0.712	0.966	0.722
High blood pressure	59%	46%	44%	0.302	0.279	0.911
Hyperlipidemia med.	15%	14%	21%	0.884	0.518	0.489
Atherosclerosis med.	2%	14%	11%	0.088	0.115	0.724
Cardiovascular med.	38%	43%	44%	0.644	0.579	0.964
Depression/anxiety med.	6%	5%	5%	0.878	0.776	0.945
Hours intellectual activity	34	33	35	0.809	0.783	0.683
Hours physical activity	21	21	25	0.853	0.252	0.375
Hours social network	27	23	29	0.211	0.421	0.100
Intensity physical act.	1.76	1.64	1.40	0.398	0.006*	0.119
Intensity intellectual act.	1.41	1.50	1.42	0.382	0.877	0.543

Note. n is 99 for class 1, 42 for class 2, and 40 for class 3. Med. = medication, act. = activity; *P <0.05.

between classes 3 and 1 on education remains statistically significant.

Genetic Differences

We next examined differences among the 3 classes on the gene score for dopamine transmission. Here, both the class with high receptor availability and low cognition (class 3; mean = 1.93; SE = 0.16) and the class with low receptor availability and low cognition (class 2; mean = 1.99; SE = 0.13) tended to score lower than class 1 (mean = 2.32; SE = 0.09; class 3 vs. 1: $\chi^2(1) = 3.92$, $P = 0.048$; class 2 vs. 1: $\chi^2(1) = 3.62$, $P = 0.057$), with no statistically significant differences between classes 2 and 3 ($\chi^2(1) = 0.8$, $P = 0.783$). Thus, genetics related to lower dopamine transmission were related to lower cognitive performance, but did not map directly onto the differences in $D_{2/3}R$ availability. There were no statistically significant differences between the classes on ApoE ε4 status. Note also that with strict Bonferroni correction for multiple testing (0.05/6 tests ≈ 0.008) none of the differences remain statistically significant.

Structural Brain Differences

Given that lower dopamine $D_{2/3}R$ availability cannot account for the low cognitive performance of individuals in class 3, we investigated differences among the classes on structural brain variables that may be indicative of general brain integrity in this cohort. Similar to the gene score, both class 2 and 3 showed smaller total gray-matter volume (adjusted for ICV) than class 1 (class 3 vs. 1: $\chi^2(1) = 5.7$, $P = 0.017$, class 2 vs. 1: $\chi^2(1) = 11.6$, $P < 0.001$). There were no statistically significant differences between classes 2 and 3, but, if anything, class 3 tended to have slightly more gray matter than class 2 (see Fig. 2A). Estimates of striatal volume followed a similar pattern, with class 1 tending to have higher striatal volume than class 2 ($\chi^2(1) = 2.5$, $P = 0.11$) and 3 ($\chi^2(1) = 3.7$, $P = 0.055$), but with no difference ($P = 0.97$) between classes 2 and 3. Cerebral blood flow in total gray matter also showed a similar pattern (Fig. 2B), with class 2 showing significantly lower flow than class 1 ($\chi^2(1) = 11.4$, $P < 0.001$), but with class 3 taking a clearer intermediate position, tending to show lower blood flow than class 1 ($\chi^2(1) = 2.7$, $P = 0.098$). The difference between classes 2 and 3 was not statistically significant ($\chi^2(1) = 2.3$, $P = 0.131$). Total burden of white-matter hyperintensities (Fig. 2C) was significantly higher in class 2 than in the other 2 classes (class 2 vs. 1: $\chi^2(1) = 9.1$, $P = 0.003$. Class 2 vs. 3: $\chi^2(1) = 5.7$, $P = 0.017$), with no statistically significant differences between classes 1 and 3 ($\chi^2(1) = 0.1$, $P = 0.722$). There were no statistically significant differences among the classes on any of the DTI variables. Thus, worse global brain integrity does not single out the class with low cognition and high receptor availability (class 3) from individuals with low performance and low receptor availability (class 2). Note also that with a stricter threshold for significance ($P < 0.001$), only the difference between classes 1 and 2 in total gray-matter volume remains significant.

Differences in Functional Brain Activity Among Classes

For striatal BP_{ND}, we noted that differences among classes portray an inverted u-shaped relation to cognitive performance, with the group having intermediate striatal BP_{ND} performing best. This conclusion is tempting to draw but perhaps overly simplistic, especially in light of earlier analyses of this data set, which did not reveal any indications of such nonlinearity

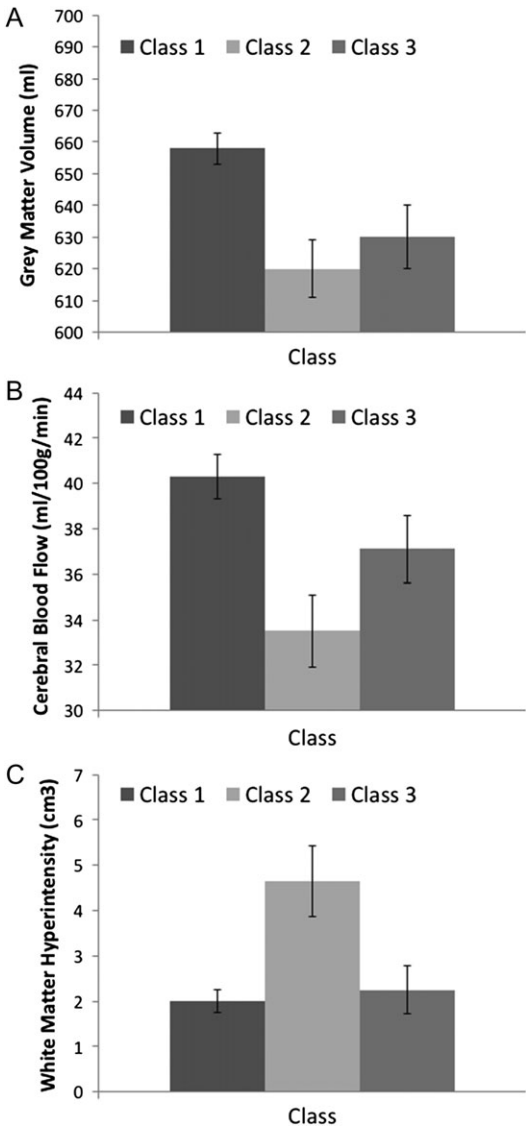

Figure 2. Mean (SE) total gray matter volume (A), mean (SE) cerebral blood flow in total gray matter (B), and mean (SE) total burden of white matter hyperintensities (C) as a function of class.

(Nyberg et al. 2016). We further note that the latent-profile model is set up to explain also the multivariate associations within the BP_{ND} and cognition domains with the formation of these classes. That is, a key addition to the solution is probably that class 3 has particularly high dopamine $D_{2/3}R$ availability in striatum relative to other regions and that this is related to especially low working memory performance relative to other cognitive functions. With this in mind, we reasoned that class 3 may have impaired working memory performance due to dysfunctional signaling between the striatum and cortex and therefore probed differences among the classes in connectivity between the caudate and the ROIs in the fronto-parietal network during rest (Fig. 3).

Class 3 had on average lower connectivity between left caudate and left DLPFC (class 3 vs. 1: $\chi^2(1) = 10.2$, $P < 0.001$; Class 3 vs. 2: $\chi^2(1) = 6.7$, $P = .010$) and between left caudate and right DLPFC (class 3 vs. 1: $\chi^2(1) = 11.4$, $P < .001$; Class 3 vs. 2: $\chi^2(1) = 9.0$, $P = 0.003$) than the other 2 classes. The results were similar for the right caudate (left DLPFC: class 3 vs. 1: $\chi^2(1) = 7.6$,

$P = 0.006$; Class 3 vs. 2: $\chi^2(1) = 5.3$, $P = 0.022$; right DLPFC: class 3 vs. 1: $\chi^2(1) = 11.3$, $P < 0.001$; Class 3 vs. 2: $\chi^2(1) = 3.8$, $P = .050$). There were no statistically significant differences between classes 1 and 2 in this regard (all $Ps > 0.171$). Several of the differences in connectivity remain statistically significant after strict Bonferroni correction for multiple testing (0.05/42 tests ≈ 0.001). The general pattern was similar for connectivity between the left caudate and the left anterior parietal cortex (class 3 vs. 1: $\chi^2(1) = 8.1$, $P = 0.004$; class 3 vs. 2: $\chi^2(1) = 7.3$, $P = 0.007$; class 1 vs. 2: $\chi^2(1) = 0.1$, $P = 0.726$). With the exception of a small difference between classes 3 and 1 for connectivity between left caudate and left anterior prefrontal cortex ($\chi^2(1) = 4.34$, $P = 0.037$) and a difference between classes 2 and 3 for connectivity between the right caudate and ACC ($\chi^2(1) = 5.14$, $P = 0.023$), no other difference between the groups reached statistical significance at the $P = 0.05$ level (all $Ps > .079$). In summary, class 3 that displayed relatively high dopamine $D_{2/3}$R availability, but low cognitive performance, shows lower connectivity of the caudate with the DLPFC bilaterally.

This pattern contrasts with the differences among classes in frontoparietal up-regulation of activity from the 1-back to the 2-back and 3-back working memory conditions. Here, both classes 2 and 3 failed to upregulate their activity (Fig. 4). Specifically, for both contrasts, class 1 showed greater upregulation than both class 2 ($\chi^2(1) = 12.6$, $P < 0.001$ and $\chi^2(1) = 16.7$, $P < 0.001$) and class 3 ($\chi^2(1) = 27.6$, $P < 0.001$ and $\chi^2(1) = 10.9$, $P < 0.001$). These differences also survive a more stringent threshold for statistical significance at $P = 0.008$ (0.05/6 tests). At the $P < 0.05$ level, there was also statistically significant difference between classes 2 and 3 for the 2-back > 1-back contrast ($\chi^2(1) = 4.5$, $P = 0.033$), but no difference between these 2 classes for the 3-back > 1-back contrast ($P = 0.94$). There were no statistically significant differences among the classes for 1-back (vs. baseline) activity (all $Ps > 0.55$).

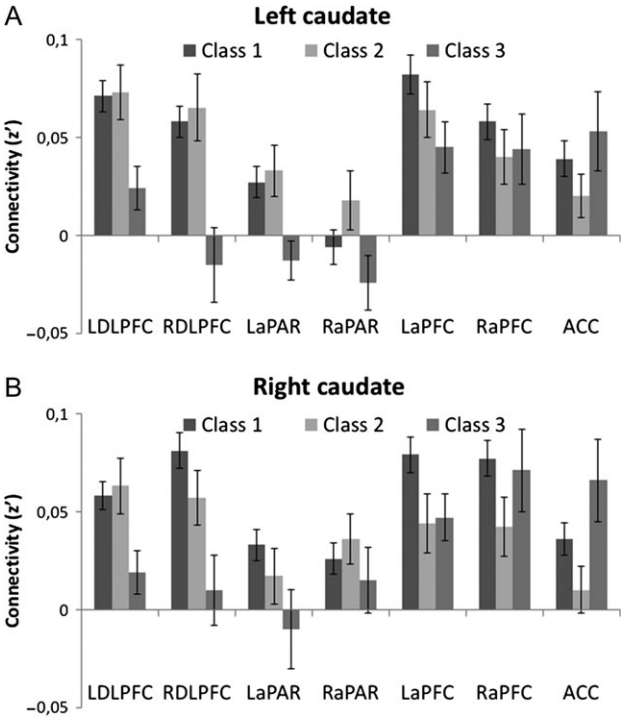

Figure 3. Mean (SE) connectivity at rest between activity in left (A) and right (B) dorsal caudate nucleus and regions-of-interest in the fronto-parietal network as a function of class. L = Left; R = Right; DLPFC = DorsoLateral Prefrontal Cortex; aPAR = anterior Parietal lobe; aPFC = anterior Prefrontal Cortex; ACC = Anterior Cingulate Cortex.

Discussion

We report a representation of the multivariate associations between dopamine $D_{2/3}$R availability and cognitive performance in a large sample of older adults with 3 classes of individuals. One of these classes is a large group of individuals with relatively high cognitive performance and $D_{2/3}$R availability. A second class of individuals performs on average lower and has relatively low $D_{2/3}$R availability. Notably, a third class displayed high $D_{2/3}$R availability, especially in the striatum, along with low cognitive performance, particularly for working memory. Put differently, relatively high $D_{2/3}$R availability was associated with high cognitive performance for most individuals, but there was a smaller group of individuals where high availability, particularly in striatum, instead came with poor performance, especially for working memory. The presence of this third class affects $D_{2/3}$R availability-cognition correlations at whole-sample level. If we were to remove this group of individuals, the mean differences between the other 2 groups would result in a positive association between dopamine $D_{2/3}$R availability and cognitive performance in general, not only for episodic memory (cf. Nyberg et al. 2016).

High dopamine $D_{2/3}$R availability in the striatum has been linked to functional impairments, particularly in working memory and related executive functions, in some groups of

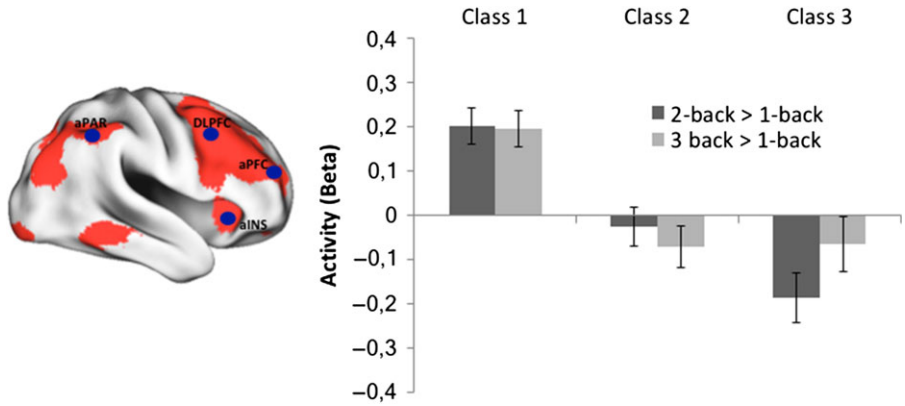

Figure 4. Mean (SE) activity (2-back vs. 1-back and 3-back vs. 1-back) averaged across the regions of the frontoparietal network as a function of class.

individuals. For example, individuals with ADHD display higher striatal $D_{2/3}R$ availability than controls, which may be related to behavioral symptoms (Lou et al. 2004; Badgaiyan et al. 2015). The evidence is similar for schizophrenia, in particular with respect to increased striatal $D_{2/3}R$ availability (Howes and Kapur 2009). Although the present sample consists of healthy normal (older) adults, we note that class 3, with the profile of cognitive performance and dopamine $D_{2/3}R$ availability that resembles these psychiatric conditions, also tended to have lower education and higher BMI than the other 2 classes—variables that often relate to psychiatric disease (Barnett et al. 2006; Gurpegui et al. 2012; Cerimele and Katon 2013; Esch et al. 2014). In particular low education, which generally is a powerful correlate of cognitive performance in both younger and older age, may play an important role in our findings: One way to summarize the findings is that performance on cognitive tests may be relatively poor, despite relatively high receptor availability, if education is low (i.e., for higher and comparable levels of education, the availability-performance association in more monotonic). The association with BMI converge well with evidence of higher dopamine $D_{2/3}R$ availability in overweight adults (but perhaps not obesity; Wang et al. 2001; Cosgrove et al. 2015; Horstmann et al. 2015; Dang et al. 2016). Given that consumption of psychotropic drugs was low in our sample and did not differ among classes, these characteristics may together be indicative of a phenotype that is associated with reduced working memory performance, regardless of psychiatric status.

It may be that individuals with such characteristics (i.e., class 3) have high receptor amount relative to their endogenous dopamine levels. This could reflect receptor upregulation that can take place upon dopamine degeneration (Brooks et al. 1992; Scherfler et al. 2006; Lin et al. 2008), but also increased ligand binding due to reduced competition with endogenous dopamine (Laruelle et al. 1997). If so, such persons may exhibit a system that is as functionally inefficient as one with few available receptors (i.e., class 2). In line with this reasoning, striatal $D_{2/3}R$ availability is normalized in ADHD following medication that increases striatal dopamine levels (Ilgin et al. 2001; Volkow et al. 2002). Furthermore, lower dopamine release relates to poorer working memory performance in schizophrenia (Rolls et al. 2008; Cassidy et al. 2016), whereas dopamine $D_{2/3}R$ availability has been found to be higher in this condition than in controls (Howes and Kapur 2009).

If relatively lower dopamine levels underlie the high $D_{2/3}R$ BP_{ND} observed in class 3, this could partly be due to genetic reasons, as this class leaned towards displaying reduced dopamine transmission gene scores when compared to class 1. Class 2 also tended to display lower dopamine transmission gene scores, but may have lower $D_{2/3}R$ availability because receptor density is correspondingly adapted. The high gene score for class 1 is in agreement with reports of higher working memory performance for beneficial allelic variants of rs4680 and rs879606 (Meyer-Lindenberg et al. 2007; Diaz-Asper et al. 2008; Lindenberger et al. 2008). An alternative explanation is that class 3 consists of individuals that have experienced particularly marked aging-related losses (relative to class 2) in dopamine release (e.g., Karlsson et al. 2009). One important aspect to consider is that affinity of ^{11}C-raclopride to the $D_{2/3}R$ varies in accordance to endogenous dopamine levels (Laruelle 2000). High BP_{ND}-values can be observed in individuals in which ligand affinity is high, presumably as a consequence to low dopamine levels (Hirvonen et al. 2009). Similarly, low BP_{ND}-values were found upon amphetamine-induced dopamine level increments, due to reduced ligand affinity (Carson et al. 2002; Doudet and Holden 2003). In such cases a high BP_{ND} is not representative of high receptor count, but rather, poor dopamine system integrity. However, with the caveat that the data are cross-sectional, the measures of total gray-matter volume, perfusion, and white matter hyperintensities suggest that class 3 is at the same level or somewhat better off in terms of general brain integrity than class 2 (although both of these classes were worse off on gray-matter volume and perfusion than the good performers in class 1).

The present results are in line with the often-observed nonmonotonic association between dopamine and working memory performance (Cools and D'Esposito 2011; Floresco 2013; Garrett et al. 2015). Although the within-person, pharmacological evidence on which this pattern is primarily based does not necessarily translate into similar between-person differences (Kievit et al. 2013; Schmiedek et al. 2016), the present analyses do (in a data-driven manner) represent the multivariate associations among the variables by forming groups consistent with a nonmonotonic dopamine-cognition association, but here with dopamine $D_{2/3}R$ availability. Notably, functional activity during the working memory task also followed this pattern, such that individuals with intermediate striatal $D_{2/3}R$ availability upregulated their frontoparietal activity across working memory load more than those with low (class 2) or high $D_{2/3}R$ availability (class 3). Moreover, the profiles suggest that such an association may be particularly pronounced for striatal dopamine $D_{2/3}R$ availability and working memory performance.

The status of striatal $D_{2/3}R$ availability in our results may relate to the strong updating component of the working memory tasks used—a cognitive process that has been linked to striatal functioning (Frank et al. 2001; Mehta et al. 2004; Dahlin et al. 2008; Bäckman et al. 2011; Cools and D'Esposito 2011; D'Ardenne et al. 2012). Striatal dopamine is thought to bias the probability of gating information into cortical representations in working memory (Frank et al. 2001; Cools and D'Esposito 2011; D'Ardenne et al. 2012). Cortical dopamine, particularly in DLPFC, may stabilize working memory representations by reducing vulnerability to interference (Durstewitz and Seamans 2008; Cools and D'Esposito 2011). These 2 processes may interact with each other in determining working memory performance, such that too much flexibility (i.e., updating) is associated with distractibility, whereas too much stability is linked to inflexibility. The balance between these 2 aspects of working memory has been suggested to depend on the circuits connecting DLPFC with the striatum (Cools and D'Esposito 2011). Our results suggest that class 3, with high $D_{2/3}R$ availability, especially in the striatum, and low performance, particularly for working memory, may have suboptimal balance in this system. Specifically, individuals in class 3 showed lower functional connectivity between dorsal caudate and DLPFC bilaterally than individuals in the 2 other groups. These results suggest that the neural circuits behind working memory are not well synchronized in class 3. Interestingly, reduced connectivity between the dorsal caudate and the fronto-parietal network has also been observed among older individuals with higher dopamine synthesis capacity (Berry et al. 2016). The similarity of these findings to the ones reported here raises the possibility that higher dopamine receptor availability may be linked to alterations in dopamine synthesis, with both perhaps emerging as responses to other changes in the dopamine system in a subset of individuals (Braskie et al. 2008; Berry et al. 2016).

The particularly strong role of relatively high striatal dopamine $D_{2/3}R$ availability in working memory, but perhaps less so

in episodic memory, is in line with our previous report of linear relationships of striatal and hippocampal dopamine $D_{2/3}$R availability to episodic memory performance (Nyberg et al. 2016). Together with theoretical and experimental work linking hippocampal dopamine receptors to episodic memory performance (Lisman et al. 2011), the present results suggest a dissociation of links of dopamine $D_{2/3}$R availability to episodic and working memory. Working memory may relate non-monotonically to $D_{2/3}$R availability, with groups of individuals characterized by low and by high striatal availability performing low, whereas episodic memory may display a more homogenous pattern of positive associations between $D_{2/3}$R availability and performance.

To substantiate our interpretations of the results, experimental work as well as longitudinal imaging work is needed. More advanced measures of $D_{2/3}$R availability than BP_{ND} measured by a single ^{11}C-raclopride-PET scan at rest would also be useful, particularly measures that allow for teasing apart receptor density and endogenous dopamine levels (Seeman et al. 1989; Yoder et al. 2008). Further, although recent evidence supports the reliability and validity of extrastriatal measurements of $D_{2/3}$R availability with ^{11}C-raclopride (Alakurtti et al. 2015; Papenberg et al. 2017), it is possible that partial-volume effects may to some degree bias the measurements. Importantly, however, we think that these measurement imperfections are unlikely to explain our main result as classes 2 and 3 did not differ much (and not statistically) in gray matter volume. We also note that the present data-analytic approach probabilistically assigns individuals to classes, and that classification accuracy was far from perfect. Hence, the groups identified in our analyses are unlikely to represent distinct entities. Rather, they can be thought of as guideposts for detecting non-linear multivariate associations that apply to the entire population (Bauer 2007). Finally, we emphasize again that the methodological approach of the current study is exploratory in nature. This also holds for the investigation of differences among the classes on other variables than those included in the latent-profile analysis. It is our aim to provide a comprehensive and broad description of classes of individuals, without attaching too much meaning to the individual comparisons of different variables between classes. That said, it should be noted that not all of the discussed differences survive p-threshold correction for multiple testing. Future confirmatory work is therefore warranted.

We have reported a data-driven representation of the associations between $D_{2/3}$R availability and cognitive performance in a large sample of older individuals with 3 subgroups of individuals. Our results emphasize the need to take into account the multivariate heterogeneity of individual profiles of $D_{2/3}$R availability and cognitive performance for understanding between-person differences in brain-cognition associations. Relatively high dopamine $D_{2/3}$R availability comes with high cognitive performance for most individuals, but there is a smaller group of individuals where high availability, especially in the striatum, instead comes with poor performance, particularly for working memory.

Supplementary Material

Supplementary data are available at *Cerebral Cortex* online.

Funding

This work was supported by the Swedish Research Council (446-2013-7189), FORTE (2013-2277), Umeå University, the Umeå University-Karolinska Institute Strategic Neuroscience program, Knut and Alice Wallenberg Foundation, Torsten Söderberg Foundation, Ragnar Söderberg Foundation, an Alexander von Humboldt Research award, a donation of the Jochnick Foundation, Swedish Brain Power, Swedish Brain Foundation, Västerbotten County Council, the Innovation Fund of the Max Planck Society, the Gottfried Wilhelm Leibniz Research Award 2010 of the German Research Foundation (DFG), the Emmy Nöther Programme from the DFG, and the Swedish National Infrastructure for Computing (SNIC) through the Abisko computer cluster at Umeå University.

Notes

Thanks to Mats Eriksson and Kajsa Burström, the research nurses who recruited and guided all participants through the complete study test battery, and all staff at UFBI. *Conflict of Interest*: None declared.

References

Alakurtti K, Johansson JJ, Joutsa J, Laine M, Backman L, Nyberg L, Rinne JO. 2015. Long-term test-retest reliability of striatal and extrastriatal dopamine D2/3 receptor binding: study with [(11)C]raclopride and high-resolution PET. J Cereb Blood Flow Metab. 35:1199–1205.

Arnsten AF. 1997. Catecholamine regulation of the prefrontal cortex. J Psychopharmacol. 11:151–162.

Arnsten AF, Cai JX, Murphy BL, Goldman-Rakic PS. 1994. Dopamine D1 receptor mechanisms in the cognitive performance of young adult and aged monkeys. Psychopharmacology (Berl). 116:143–151.

Ashburner J. 2007. A fast diffeomorphic image registration algorithm. Neuroimage. 38:95–113.

Ashburner J, Friston K. 2005. Unified segmentation. Neuroimage. 26:839–851.

Backman L, Nyberg L, Lindenberger U, Li SC, Farde L. 2006. The correlative triad among aging, dopamine, and cognition: current status and future prospects. Neurosci Biobehav R. 30:791–807.

Badgaiyan RD, Sinha S, Sajjad M, Wack DS. 2015. Attenuated tonic and enhanced phasic release of dopamine in attention deficit hyperactivity disorder. Plos One. 10:e0137326.

Bakk Z, Vermunt JK. 2015. Robustness of stepwise latent class modeling with continuous distal outcomes. Structural Equation Modeling. 23:20–31.

Barnett JH, Salmond CH, Jones PB, Sahakian BJ. 2006. Cognitive reserve in neuropsychiatry. Psychol Med. 36:1053–1064.

Bauer DJ. 2007. Observations on the use of growth mixture models in psychological research. Multivar Behav Res. 42: 757–786.

Berry AS, Shah VD, Baker SL, Vogel JW, O'Neil JP, Janabi M, Schwimmer HD, Marks SM, Jagust WJ. 2016. Aging Affects Dopaminergic Neural Mechanisms of Cognitive Flexibility. J Neurosci. 36:12559–12569.

Bettinardi V, Presotto L, Rapisarda E, Picchio M, Gianolli L, Gilardi MC. 2011. Physical performance of the new hybrid PETCT Discovery-690. Med Phys. 38:5394–5411.

Braskie MN, Wilcox CE, Landau SM, O'Neil JP, Baker SL, Madison CM, Kluth JT, Jagust WJ. 2008. Relationship of striatal dopamine synthesis capacity to age and cognition. J Neurosci. 28: 14320–14328.

Brooks DJ, Ibanez V, Sawle GV, Playford ED, Quinn N, Mathias CJ, Lees AJ, Marsden CD, Bannister R, Frackowiak RS. 1992.

Striatal D2 receptor status in patients with Parkinson's disease, striatonigral degeneration, and progressive supranuclear palsy, measured with 11C-raclopride and positron emission tomography. Ann Neurol. 31:184–192.

Bäckman L, Lindenberger U, Li SC, Nyberg L. 2010. Linking cognitive aging to alterations in dopamine neurotransmitter functioning: Recent data and future avenues. Neurosci Biobehav R. 34:670–677.

Bäckman L, Nyberg L, Soveri A, Johansson J, Andersson M, Dahlin E, Neely AS, Virta J, Laine M, Rinne JO. 2011. Effects of working-memory training on striatal dopamine release. Science. 333:718.

Carson RE, Channing MA, Der MG, Herscovitch P, Eckelman WC. 2002. Scatchard analysis with bolus/infusion administration of [C-11]raclopride: amphetamine effects in anesthetized monkeys. In: Senda M, Kimura Y, Herscovitch P, editors. Brain imaging using PET. San Diego, CA: Academic Press. p. 63–69.

Cassidy CM, Van Snellenberg JX, Benavides C, Slifstein M, Wang Z, Moore H, Abi-Dargham A, Horga G. 2016. Dynamic Connectivity between Brain Networks Supports Working Memory: Relationships to Dopamine Release and Schizophrenia. J Neurosci. 36:4377–4388.

Cerimele JM, Katon WJ. 2013. Associations between health risk behaviors and symptoms of schizophrenia and bipolar disorder: a systematic review. Gen Hosp Psychiatry. 35:16–22.

Chao-Gan Y, Yu-Feng Z. 2010. DPARSF: A MATLAB Toolbox for "Pipeline" Data Analysis of Resting-State fMRI. Front Syst Neurosci. 4:13.

Christensen H, Batterham PJ, Mackinnon AJ, Jorm AF, Mack HA, Mather KA, Anstey KJ, Sachdev PS, Easteal S. 2008. The association of APOE genotype and cognitive decline in interaction with risk factors in a 65–69 year old community sample. BMC Geriatr. 8:14.

Colzato LS, Steenbergen L, Sellaro R, Stock AK, Arning L, Beste C. 2016. Effects of l-Tyrosine on working memory and inhibitory control are determined by DRD2 genotypes: A randomized controlled trial. Cortex. 82:217–224.

Cools R, D'Esposito M. 2011. Inverted-U-shaped dopamine actions on human working memory and cognitive control. Biol Psychiatry. 69:e113–e125.

Cosgrove KP, Veldhuizen MG, Sandiego CM, Morris ED, Small DM. 2015. Opposing relationships of BMI with BOLD and dopamine D2/3 receptor binding potential in the dorsal striatum. Synapse. 69:195–202.

D'Ardenne K, Eshel N, Luka J, Lenartowicz A, Nystrom LE, Cohen JD. 2012. Role of prefrontal cortex and the midbrain dopamine system in working memory updating. Proc Natl Acad Sci USA. 109:19900–19909.

Dahlin E, Neely AS, Larsson A, Backman L, Nyberg L. 2008. Transfer of learning after updating training mediated by the striatum. Science. 320:1510–1512.

Dang LC, Samanez-Larkin GR, Castrellon JJ, Perkins SF, Cowan RL, Zald DH. 2016. Associations between dopamine D2 receptor availability and BMI depend on age. Neuroimage. 138:176–183.

Desikan RS, Segonne F, Fischl B, Quinn BT, Dickerson BC, Blacker D, Buckner RL, Dale AM, Maguire RP, Hyman BT, et al. 2006. An automated labeling system for subdividing the human cerebral cortex on MRI scans into gyral based regions of interest. Neuroimage. 31:968–980.

Di Martino A, Scheres A, Margulies DS, Kelly AM, Uddin LQ, Shehzad Z, Biswal B, Walters JR, Castellanos FX, Milham MP. 2008. Functional connectivity of human striatum: a resting state FMRI study. Cereb Cortex. 18:2735–2747.

Diaz-Asper CM, Goldberg TE, Kolachana BS, Straub RE, Egan MF, Weinberger DR. 2008. Genetic variation in catechol-O-methyltransferase: effects on working memory in schizophrenic patients, their siblings, and healthy controls. Biol Psychiatry. 63:72–79.

Doudet DJ, Holden JE. 2003. Raclopride studies of dopamine release: dependence on presynaptic integrity. Biol Psychiatry. 54:1193–1199.

Durstewitz D, Seamans JK. 2008. The dual-state theory of prefrontal cortex dopamine function with relevance to catechol-o-methyltransferase genotypes and schizophrenia. Biol Psychiatry. 64:739–749.

Esch P, Bocquet V, Pull C, Couffignal S, Lehnert T, Graas M, Fond-Harmant L, Ansseau M. 2014. The downward spiral of mental disorders and educational attainment: a systematic review on early school leaving. Bmc Psychiatry. 14:237.

Farde L, Hall H, Ehrin E, Sedvall G. 1986. Quantitative analysis of D2 dopamine receptor binding in the living human brain by PET. Science. 231:258–261.

Fischl B, Salat DH, Busa E, Albert M, Dieterich M, Haselgrove C, van der Kouwe A, Killiany R, Kennedy D, Klaveness S, et al. 2002. Whole brain segmentation: automated labeling of neuroanatomical structures in the human brain. Neuron. 33:341–355.

Floresco SB. 2013. Prefrontal dopamine and behavioral flexibility: shifting from an "inverted-U" toward a family of functions. Front Neurosci. 7:62.

Floresco SB, Magyar O, Ghods-Sharifi S, Vexelman C, Tse MT. 2006. Multiple dopamine receptor subtypes in the medial prefrontal cortex of the rat regulate set-shifting. Neuropsychopharmacol. 31:297–309.

Frank MJ, Loughry B, O'Reilly RC. 2001. Interactions between frontal cortex and basal ganglia in working memory: a computational model. Cogn Affect Behav Neurosci. 1: 137–160.

Garrett DD, Nagel IE, Preuschhof C, Burzynska AZ, Marchner J, Wiegert S, Jungehulsing GJ, Nyberg L, Villringer A, Li SC, et al. 2015. Amphetamine modulates brain signal variability and working memory in younger and older adults. Proc Natl Acad Sci USA. 112:7593–7598.

Gurpegui M, Martinez-Ortega JM, Gutierrez-Rojas L, Rivero J, Rojas C, Jurado D. 2012. Overweight and obesity in patients with bipolar disorder or schizophrenia compared with a non-psychiatric sample. Prog Neuropsychopharmacol Biol Psychiatry. 37:169–175.

Hirvonen M, Laakso A, Nagren K, Rinne JO, Pohjalainen T, Hietala J. 2004. C957T polymorphism of the dopamine D2 receptor (DRD2) gene affects striatal DRD2 availability in vivo. Mol Psychiatry. 9:1060–1061.

Hirvonen MM, Laakso A, Nagren K, Rinne JO, Pohjalainen T, Hietala J. 2009. C957T polymorphism of dopamine D2 receptor gene affects striatal DRD2 in vivo availability by changing the receptor affinity. Synapse. 63:907–912.

Hoaglin DC, Iglewicz B. 1987. Fine tuning some resistant rules for outlier labeling. J Am Statist Associat. 82:1147–1149.

Horstmann A, Fenske WK, Hankir MK. 2015. Argument for a non-linear relationship between severity of human obesity and dopaminergic tone. Obes Rev. 16:821–830.

Howes OD, Kapur S. 2009. The dopamine hypothesis of schizophrenia: version III–the final common pathway. Schizophr Bull. 35:549–562.

Ilgin N, Senol S, Gucuyener K, Gokcora N, Sener S. 2001. Is increased D2 receptor availability associated with response to stimulant medication in ADHD. Dev Med Child Neurol. 43:755–760.

Innis RB, Cunningham VJ, Delforge J, Fujita M, Gjedde A, Gunn RN, Holden J, Houle S, Huang SC, Ichise M, et al. 2007. Consensus nomenclature for in vivo imaging of reversibly binding radioligands. J Cereb Blood Flow Metab. 27: 1533–1539.

Jian Y, Planeta B, Carson RE. 2015. Evaluation of bias and variance in low-count OSEM list mode reconstruction. Phy Med Biol. 60:15–29.

Karlsson S, Nyberg L, Karlsson P, Fischer H, Thilers P, Macdonald S, Brehmer Y, Rieckmann A, Halldin C, Farde L, et al. 2009. Modulation of striatal dopamine D1 binding by cognitive processing. Neuroimage. 48:398–404.

Kievit RA, Frankenhuis WE, Waldorp LJ, Borsboom D. 2013. Simpson's paradox in psychological science: a practical guide. Frontiers in psychology. 4:513.

Kunii Y, Hyde TM, Ye T, Li C, Kolachana B, Dickinson D, Weinberger DR, Kleinman JE, Lipska BK. 2014. Revisiting DARPP-32 in postmortem human brain: changes in schizophrenia and bipolar disorder and genetic associations with t-DARPP-32 expression. Mol Psychiatry. 19:192–199.

Lachman HM, Papolos DF, Saito T, Yu YM, Szumlanski CL, Weinshilboum RM. 1996. Human catechol-O-methyltransferase pharmacogenetics: description of a functional polymorphism and its potential application to neuropsychiatric disorders. Pharmacogenetics. 6:243–250.

Lanza ST, Tan X, Bray BC. 2013. Latent class analysis with distal outcomes: a flexible model-based approach. Struct Equ Modeling. 20:1–26.

Laruelle M. 2000. Imaging synaptic neurotransmission with in vivo binding competition techniques: a critical review. J Cereb Blood Flow Metab. 20:423–451.

Laruelle M, D'Souza CD, Baldwin RM, Abi-Dargham A, Kanes SJ, Fingado CL, Seibyl JP, Zoghbi SS, Bowers MB, Jatlow P, et al. 1997. Imaging D2 receptor occupancy by endogenous dopamine in humans. Neuropsychopharmacol. 17:162–174.

Leemans A, Jones DK. 2009. The B-matrix must be rotated when correcting for subject motion in DTI data. Magn Reson Med. 61:1336–1349.

Levey AI, Hersch SM, Rye DB, Sunahara RK, Niznik HB, Kitt CA, Price DL, Maggio R, Brann MR, Ciliax BJ. 1993. Localization of D1 and D2 dopamine receptors in brain with subtype-specific antibodies. Proc Natl Acad Sci USA. 90:8861–8865.

Liggins JTP. 2009. The roles of dopamine D1 and D2 receptors in working memory function. MSURJ. 4:39–45.

Lin CH, Huang JY, Ching CH, Chuang JI. 2008. Melatonin reduces the neuronal loss, downregulation of dopamine transporter, and upregulation of D2 receptor in rotenone-induced parkinsonian rats. J Pineal Res. 44:205–213.

Lindenberger U, Nagel IE, Chicherio C, Li SC, Heekeren HR, Backman L. 2008. Age-related decline in brain resources modulates genetic effects on cognitive functioning. Front Neurosci. 2:234–244.

Lisman J, Grace AA, Duzel E. 2011. A neoHebbian framework for episodic memory; role of dopamine-dependent late LTP. Trends Neurosci. 34:536–547.

Logan J, Fowler JS, Volkow ND, Wang GJ, Ding YS, Alexoff DL. 1996. Distribution volume ratios without blood sampling from graphical analysis of PET data. J Cereb Blood Flow Metab. 16:834–840.

Lou HC, Rosa P, Pryds O, Karrebaek H, Lunding J, Cumming P, Gjedde A. 2004. ADHD: increased dopamine receptor availability linked to attention deficit and low neonatal cerebral blood flow. Dev Med Child Neurol. 46:179–183.

Luciana M, Depue RA, Arbisi P, Leon A. 1992. Facilitation of working memory in humans by a d2 dopamine receptor agonist. J Cogn Neurosci. 4:58–68.

Mehta MA, Manes FF, Magnolfi G, Sahakian BJ, Robbins TW. 2004. Impaired set-shifting and dissociable effects on tests of spatial working memory following the dopamine D2 receptor antagonist sulpiride in human volunteers. Psychopharmacology (Berl). 176:331–342.

Meyer-Lindenberg A, Straub RE, Lipska BK, Verchinski BA, Goldberg T, Callicott JH, Egan MF, Huffaker SS, Mattay VS, Kolachana B, et al. 2007. Genetic evidence implicating DARPP-32 in human frontostriatal structure, function, and cognition. J Clin Invest. 117:672–682.

Muthén LK, Muthén BO. 2015. Mplus user's guide. Los Angeles, CA: Muthen & Muthen.

Nevalainen N, Riklund K, Andersson M, Axelsson J, Ogren M, Lovden M, Lindenberger U, Backman L, Nyberg L. 2015. COBRA: A prospective multimodal imaging study of dopamine, brain structure and function, and cognition. Brain Res. 1612:83–103.

Nyberg L, Karalija N, Salami A, Andersson M, Wåhlin A, Kaboovand N, Köhncke Y, Azelsson J, Rieckmann A, Papenberg G, et al. 2016. Dopamine D2 receptor availability is linked to hippocampal-caudate functional connectivity and episodic memory. Proc Natl Acad Sci USA. 113:7918–23.

Ott T, Nieder A. 2017. Dopamine D2 receptors enhance population dynamics in primate prefrontal working memory circuits. Cereb Cortex.27:4423–4435.

Papenberg G, Jonasson L, Karalija N, Köhncke Y, Andersson MA, Axelsson J, Riklund K, Lindenberger U, Lövdén M, Nyberg L, et al. 2017. Mapping the landscape of human dopamine D2 receptors Manucript submitted for publication.

Postuma RB, Dagher A. 2006. Basal ganglia functional connectivity based on a meta-analysis of 126 positron emission tomography and functional magnetic resonance imaging publications. Cereb Cortex. 16:1508–1521.

Puig MV, Miller EK. 2015. Neural substrates of dopamine D2 receptor modulated executive functions in the monkey prefrontal cortex. Cereb Cortex. 25:2980–2987.

Rakshi JS, Uema T, Ito K, Bailey DL, Morrish PK, Ashburner J, Dagher A, Jenkins IH, Friston KJ, Brooks DJ. 1999. Frontal, midbrain and striatal dopaminergic function in early and advanced Parkinson's disease A 3D [(18)F]dopa-PET study. Brain. 122:1637–1650.

Raz N, Lindenberger U, Rodrigue KM, Kennedy KM, Head D, Williamson A, Dahle C, Gerstorf D, Acker JD. 2005. Regional brain changes in aging healthy adults: general trends, individual differences and modifiers. Cereb Cortex. 15:1676–1689.

Rieckmann A, Karlsson S, Fischer H, Backman L. 2011. Caudate dopamine D1 receptor density is associated with individual differences in frontoparietal connectivity during working memory. J Neurosci. 31:14284–14290.

Roffman JL, Tanner AS, Eryilmaz H, Rodriguez-Thompson A, Silverstein NJ, Ho NF, Nitenson AZ, Chonde DB, Greve DN, Abi-Dargham A, et al. 2016. Dopamine D1 signaling organizes network dynamics underlying working memory. Sci Adv. 2:e1501672.

Rolls ET, Loh M, Deco G, Winterer G. 2008. Computational models of schizophrenia and dopamine modulation in the prefrontal cortex. Nat Rev Neurosci. 9:696–709.

Salami A, Eriksson J, Nilsson LG, Nyberg L. 2012. Age-related white matter microstructural differences partly mediate age-related decline in processing speed but not cognition. Biochim Biophys Acta. 1822:408–415.

Scherfler C, Khan NL, Pavese N, Lees AJ, Quinn NP, Brooks DJ, Piccini PP. 2006. Upregulation of dopamine D2 receptors in dopaminergic drug-naive patients with Parkin gene mutations. Mov Disord. 21:783–788.

Schiepers OJ, Harris SE, Gow AJ, Pattie A, Brett CE, Starr JM, Deary IJ. 2012. APOE E4 status predicts age-related cognitive decline in the ninth decade: longitudinal follow-up of the Lothian Birth Cohort 1921. Mol Psychiatry. 17:315–324.

Schmidt P, Gaser C, Arsic M, Buck D, Forschler A, Berthele A, Hoshi M, Ilg R, Schmid VJ, Zimmer C, et al. 2012. An automated tool for detection of FLAIR-hyperintense white-matter lesions in Multiple Sclerosis. Neuroimage. 59:3774–3783.

Schmiedek F, Lövdén M, von Oertzen T, Lindenberger U 2016. The Structure of Human Intelligence Cannot Be Inferred From Between-Person Differences. Manucript submitted for publication.

Schwab SG, Franke PE, Hoefgen B, Guttenthaler V, Lichtermann D, Trixler M, Knapp M, Maier W, Wildenauer DB. 2005. Association of DNA polymorphisms in the synaptic vesicular amine transporter gene (SLC18A2) with alcohol and nicotine dependence. Neuropsychopharmacol. 30:2263–2268.

Seeman P, Guan HC, Niznik HB. 1989. Endogenous dopamine lowers the dopamine D2 receptor density as measured by [3H]raclopride: implications for positron emission tomography of the human brain. Synapse. 3:96–97.

Shohamy D, Adcock RA. 2010. Dopamine and adaptive memory. Trends Cogn Sci. 14:464–472.

Smith SM. 2002. Fast robust automated brain extraction. Hum Brain Mapp. 17:143–155.

Takahashi H. 2013. PET neuroimaging of extrastriatal dopamine receptors and prefrontal cortex functions. J Physiol. 107: 503–509.

Takahashi H, Kato M, Takano H, Arakawa R, Okumura M, Otsuka T, Kodaka F, Hayashi M, Okubo Y, Ito H, et al. 2008. Differential contributions of prefrontal and hippocampal dopamine D-1 and D-2 receptors in human cognitive functions. J Neurosci. 28:12032–12038.

van Holstein M, Aarts E, van der Schaaf ME, Geurts DE, Verkes RJ, Franke B, van Schouwenburg MR, Cools R. 2011. Human cognitive flexibility depends on dopamine D2 receptor signaling. Psychopharmacology (Berl). 218:567–578.

Vincent JL, Kahn I, Snyder AZ, Raichle ME, Buckner RL. 2008. Evidence for a frontoparietal control system revealed by intrinsic functional connectivity. J Neurophysiol. 100: 3328–3342.

Volkow ND, Wang GJ, Fowler JS, Logan J, Franceschi D, Maynard L, Ding YS, Gatley SJ, Gifford A, Zhu W, et al. 2002. Relationship between blockade of dopamine transporters by oral methylphenidate and the increases in extracellular dopamine: therapeutic implications. Synapse. 43:181–187.

Wakana S, Jiang HY, Nagae-Poetscher LM, van Zijl PCM, Mori S. 2004. Fiber tract-based atlas of human white matter anatomy. Radiology. 230:77–87.

Walker MD, Asselin MC, Julyan PJ, Feldmann M, Talbot PS, Jones T, Matthews JC. 2011. Bias in iterative reconstruction of low-statistics PET data: benefits of a resolution model. Phys Med Biol. 56:931–949.

Wallsten E, Axelsson J, Sundstrom T, Riklund K, Larsson A. 2013. Subcentimeter tumor lesion delineation for high-resolution 18 F-FDG PET images: optimizing correction for partial-volume effects. J Nucl Med Technol. 41:85–91.

Wang GJ, Volkow ND, Logan J, Pappas NR, Wong CT, Zhu W, Netusil N, Fowler JS. 2001. Brain dopamine and obesity. Lancet. 357:354–357.

Yan CG, Craddock RC, He Y, Milham MP. 2013. Addressing head motion dependencies for small-world topologies in functional connectomics. Front Hum Neurosci. 7:910.

Yoder KK, Kareken DA, Morris ED. 2008. What were they thinking? Cognitive states may influence [11 C]raclopride binding potential in the striatum. Neurosci Lett. 430:38–42.

Zahrt J, Taylor JR, Mathew RG, Arnsten AF. 1997. Supranormal stimulation of D1 dopamine receptors in the rodent prefrontal cortex impairs spatial working memory performance. J Neurosci. 17:8528–8535.